Signature of Low-Dimensional Diffusion in Complex Systems

N. Malikova,* S. Longeville, and J.-M. Zanotti
Laboratoire Léon Brillouin, UMR CEA-CNRS 12, CEA Saclay, 91191 Gif-sur-Yvette, France

E. Dubois, V. Marry, and P. Turq
Université Pierre et Marie Curie - Paris 6, UMR-UPMC-CNRS-ESPCI 7612, Laboratoire LI2C, Case 51, 4 place Jussieu, Paris F-75252, France

J. Ollivier
Institut Laue-Langevin, Avenue des Martyrs-BP 156, 38042 Grenoble Cedex 9, France
(Received 22 July 2008; published 22 December 2008)

We present a clear signature of the dimensionality of water diffusion in a powder sample of a synthetic hectorite (a model clay), by analyzing the corresponding neutron scattering functions. The data follow the theoretical predictions for a powder-averaged two-dimensional diffusion, with a two-dimensional diffusion coefficient of 0.75×10^{-9} $m^2 s^{-1}$. Neutron scattering data of bulk water are used as a reference, representing motion in three dimensions. The approach is based on analyzing the scattered intensity at zero energy transfers, along with the broadening of the scattering functions, collected at a wide range of energy resolutions. The mathematical relationship between these two quantities follows, for a given shape of the resolution function, a universal master curve, independent of the diffusion coefficient, but strongly dependent on the dimensionality of the motion, which can thus be determined with clarity.

DOI: 10.1103/PhysRevLett.101.265901 PACS numbers: 66.30.jj, 25.40.Dn, 61.43.Gt, 82.75.−z

Diffusion of individual atoms or molecules confined within materials or matrices of complex architectures lies at the heart of many physical, chemical and biological processes and its study is relevant in a whole spectrum of research fields. The intense search for new energy sources encounters this issue in the development of solid electrolytes [1,2] or efficient hydrogen storage materials (such as carbon nanotubes, e.g., [3], or metal organic frameworks, e.g., [4]). Understanding the properties of clays, the main constituents of soil with their remarkable capacities to retain and release water, salts and small organic species [5], is not only important for agriculture and environmental protection but also for issues of radioactive waste disposal. Diffusion or transport under complex geometries is essential for the immense field of catalysis. Diffusion of reactants towards an active site of a porous catalyst, such as a zeolite [6], is often the rate-determining step in the reaction kinetics. Channelling reactants between membranes or along cytoskeletal filaments towards an active site of an enzyme in the crowded environment of a cell is another example [7].

For all of the above examples, dimensionality of the atomic diffusion or transport is an essential aspect resulting from the microscopic mechanism of the process itself combined with the local geometry of the surrounding matrix or environment [7–10]. Dimensionality of diffusion has been studied widely by neutron scattering techniques, as the diffusing species of interest is very often hydrogen-containing [3,4,11]. While the theoretical forms of the scattering functions for atomic diffusion in 1, 2 or 3 dimensions are well known and distinguishable, in the majority of experimental studies this difference is too small for the dimensionality to be determined with confidence [12,13]. This is due to the finite energy resolution and above all due to the physical nature of the samples themselves, which almost always come in the form of a powder. Powder nature of most of the above-mentioned systems lies at the heart of their applications, as it increases the accessible surface area of the matrix. Using bulk water and water molecules diffusing within the pores of a synthetic clay, we present here measurements of neutron scattering functions and their analysis which allows us to overcome the experimental difficulty linked to the ''powder-averaged'' low-dimensional scattering functions and determine clearly the dimensionality of diffusion.

Synthetic hectorite, as many clays, comes in a powder form. However, each grain of the powder is a highly regular stack of crystalline aluminosilicate layers (each layer is under 1 nm thick and extending over 100 s of nm in the lateral dimensions). The regular stacking distance, also called the interlayer spacing, gives rise to a series of distinct Bragg peaks [5]. Discrete layers of water are incorporated between adjacent clay layers, when the system is exposed to increased humidity. As a result, the interlayer spacing increases. (The driving force of this phenomenon is the hydration of cations present between the negatively charged clay layers [14].) The synthetic hectorite sample used here has a very-well defined structure and distinct hydration states, unlike its natural clay counterparts [15]. It was equilibrated under an atmosphere of 85% relative humidity, resulting in an interlayer spacing of 15.5 Å. This corresponds to two layers of water, with an

overall thickness of approximately 6 Å, confined between adjacent aluminosilicate layers [16]. All this structural information therefore suggests a powder-averaged two-dimensional motion for water confined in a powder sample of a hectorite clay.

For both hydrated clay and bulk water, we probed the self-diffusion of hydrogen atoms (constituents of water molecules) by measuring their strong incoherent neutron scattering signal, which dominates in the chosen wave-vector range ($Q < 1.0$ Å^{-1}). This high limit of Q was chosen such that the motion of hydrogen atoms can be treated as primarily translational. (At higher Q rotational motion and, possibly, effects of jump diffusion become significant [17–19].) For clay data, a low Q limit of 0.6 Å^{-1} was set by the appearance of a Bragg peak (coherent signal) from the clay sample (peak at 0.4–0.5 Å^{-1} reflecting the interlayer spacing). The measurements of $S(Q, \omega)$ were carried out on the time-of-flight neutron scattering spectrometer IN5B (Institut Laue Langevin, Grenoble, France [20]) at room temperature and pressure. The resolution function, the shape of which is Gaussian on IN5B, was varied between $H_G = 150$ μeV and $H_G = 5$ μeV (where H_G is the HWHM of the Gaussian resolution function). Q-summation was carried out over an increasing number of detectors, as the incident neutron wavelength increased to achieve a higher resolution. The contribution of water to $S(Q, \omega)$ was obtained after subtraction of purely elastic contributions: sample cell and, for hectorite, signal from the dry clay. The latter represents only 5%–8% of the total scattered intensity of the hydrated clay, as the hectorite used contains no structural hydrogen atoms [15].

We recall that, for a time-dependent self-correlation function, $G_s(\mathbf{r}, t)$, of a Gaussian shape, the general expression for the single particle (or incoherent) scattering function, $S_{\mathrm{inc}}(\mathbf{Q}, \omega)$, is a Lorentzian. The two are related by a double Fourier transform, in $\mathbf{r}$ and t. (For convenience, we use from now on the expression for the scattering function with ω denoting an energy transfer rather than frequency.) The scattering functions corresponding to one-, two- and three-dimensional (1D, 2D, 3D) single particle motion can be all expressed as different limits of the following expression [17,21]

$$S_{\mathrm{inc}}(\mathbf{Q}, \omega) = \frac{1}{\pi} \frac{(D_{\|}\cos^2(\theta) + D_{\perp}\sin^2(\theta))Q^2}{(D_{\|}\cos^2(\theta) + D_{\perp}\sin^2(\theta))^2 Q^4 + \omega^2}, \quad (1)$$

where θ is the angle of the wave-vector $\mathbf{Q}$ with respect to a chosen principal direction (defined by a unit vector $\mathbf{n}$) in the system, $D_{\|}$ and $D_{\perp}$ are the diffusion coefficients parallel and perpendicular to this direction [22]. Motion in 1D is the limit of $D_{\|} = D_{1\mathrm{D}}$ and $D_{\perp} = 0$ with $\mathbf{n}$ pointing along the direction of the 1D motion, for 2D motion $D_{\perp} = D_{2\mathrm{D}}$ and $D_{\|} = 0$, with $\mathbf{n}$ pointing along a normal to the plane of diffusion, for 3D motion $D_{\perp} = D_{\|} = D_{3\mathrm{D}}$ with the direction of $\mathbf{n}$ being irrelevant.

We consider now in more detail the case of 2D motion, similar arguments hold for 1D motion. For an atom diffusing in 2D $S_{\mathrm{inc}}(\mathbf{Q}, \omega)$ diverges for $\mathbf{Q} \| \mathbf{n}$, i.e., $S(\mathbf{Q}, \omega) = \delta(\omega = 0)$. As the direction of $\mathbf{Q}$ shifts towards being perpendicular to $\mathbf{n}$, the signal is increasingly broadened and reaches a Lorentzian of half width half maximum (HWHM) equal to $D_{\perp}Q^2$, where $\mathbf{Q}$ is now lying in the diffusion plane. The "powder-averaged" analogue of $S_{\mathrm{inc}}(\mathbf{Q}, \omega)$ is simply $\langle S_{\mathrm{inc}}(Q, \omega)\rangle_{\theta} = \frac{1}{2}\int_0^{\pi} S_{\mathrm{inc}}(\mathbf{Q}, \omega) \times \sin\theta d\theta$, where all directions of $\mathbf{Q}$ are now equivalent and thus only the dependence on Q ($= |\mathbf{Q}|$) remains [17,21]. The divergence of the signal at $\omega = 0$ is still present, as for any orientation of $\mathbf{Q}$ there are regions or grains of the sample that satisfy the condition of $\mathbf{Q} \| \mathbf{n}$. However, in an experiment, the divergence of $S(Q, 0)$ is never seen, as the signal is smeared out by the resolution function. Nevertheless, an excess elastic intensity is expected, providing the experimental resolution is sufficiently high. It is indeed possible to trace the emergence of this divergence as experimental resolution increases, as shown theoretically [23].

Let us first look at the measured scattering functions for water in clay and bulk water at the extreme resolutions used here. Figure 1 shows the experimental $S(Q, \omega)$ signals for (a) a low resolution ($H_G = 100$ μeV or FWHM = 200 μeV) and (b) a high resolution ($H_G = 5$ μeV or FWHM = 10 μeV). Resolution functions are shown explicitly in each case. At low resolution, the quasielastic broadening of both data sets can be modeled using the isotropic (3D) model of $S(Q, \omega)$, with the well-known 3D diffusion coefficient 2.3×10^{-9} m^2 s^{-1} in the case of bulk water and $D_{3\mathrm{D}} = 0.45 \times 10^{-9}$ m^2 s^{-1} in the case of water in clays [16]. At high resolution, the appearance of significant intensity at zero energy transfers in case of water in the clay is easily seen (Fig. 1 bottom). As is shown, a powder-averaged 2D model (with $D_{\perp} = D_{2\mathrm{D}} = 0.75 \times 10^{-9}$ m^2 s^{-1}) can account for it. (The error in these diffusion coefficients is less than 0.1×10^{-9} m^2 s^{-1}.) Modeling the high resolution clay data with a 3D model, requires an extra elastic peak. This could be interpreted as originating from a subfamily of immobile water molecules, while the rest undergoes a 3D motion. This type of conclusion, here erroneous, can be easily drawn from scattering functions measured at an insufficient resolution. The importance of a test at several resolutions (and the use of more than one scattering technique) is clear. In the case of synthetic hectorite clay, we possess information from another scattering technique (neutron spin echo), which shows that water in the system is well characterized by a single relaxation time and that at the resolution of $H_G = 5$ μeV, all water molecules should be seen as mobile [16]. We suggest therefore that the increased intensity at zero energy transfers seen for water in hectorite at this high resolution is connected to the low-dimensional nature of water diffusion in the system. Is there a way of providing a more compelling evidence for this? We present it in the

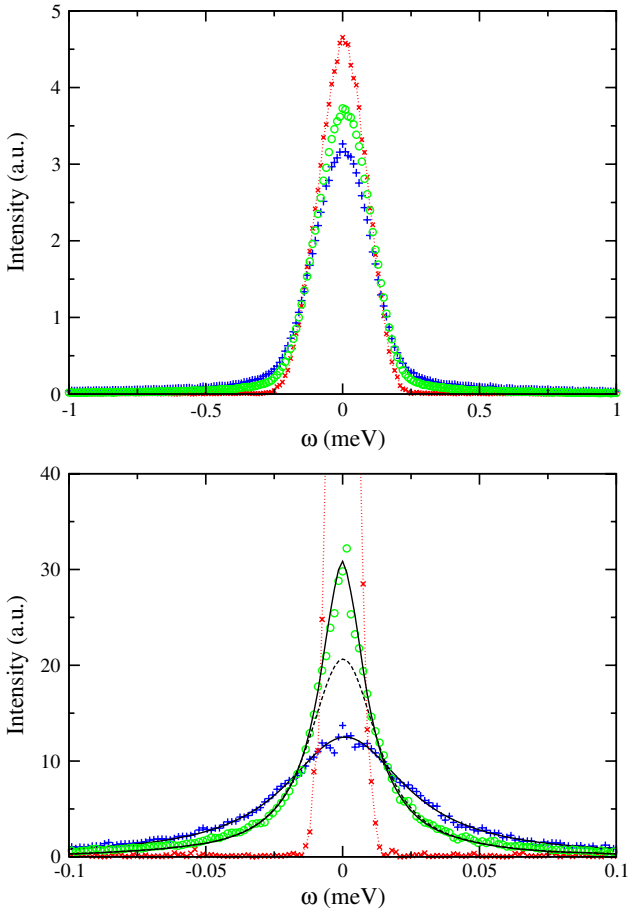

FIG. 1 (color online). $S(Q, \omega)$ (normalized) for water in clay (green ○) and bulk water (blue +). Resolution function is shown in red ×. Top: At this low resolution ($H_G = 100$ μeV), the broadening of the diffusive process, $D_{n\mathrm{D}}Q^2$, accounts only for 15%–20% of ($D_{n\mathrm{D}}Q^2 + H_G$). Both signals, bulk water and water in clay can be accounted for by a 3D model. Bottom: At this high resolution ($H_G = 5$ μeV) $D_{n\mathrm{D}}Q^2$ accounts for 70%–80% of ($D_{n\mathrm{D}}Q^2 + H_G$). Bulk water data are accounted for by a 3D model (black line), while the signal from water in clay can only be explained using a powder-averaged 2D model (black line). A 3D model applied to the data from clay (dashed black line) requires an explicit extra elastic intensity. At both resolutions, bulk water signal is shown at $Q = 0.4$ Å^{-1}, water in clay at $Q = 0.6$ Å^{-1}, to yield a comparable $D_{n\mathrm{D}}Q^2$.

remainder of the Letter, the evidence is based on a simultaneous analysis of scattering functions at a wide range of experimental resolutions.

Let us consider in more detail the dependence of the observed elastic intensity at a fixed Q and as a function of increasing experimental resolution [23]. This method relies on an initial estimate of the diffusion coefficient in the system ($D_{n\mathrm{D}}$, diffusion coefficient in n dimensions). For a given wave-vector Q we define a broad range of resolutions, such that the ratio (α) defined as $D_{n\mathrm{D}}Q^2/(D_{n\mathrm{D}}Q^2 + H)$ spans the range of 0 to 1, where $D_{n\mathrm{D}}Q^2$ is related to the HWHM broadening from the diffusive process, and H is the HWHM of the resolution function, $R(\omega)$. These two limits of course correspond to the resolution function of infinite and zero H, respectively. At each resolution the quantity of interest is the value of the normalized experimentally observed $S(Q, \omega)$ at $\omega = 0$, i.e. $S(Q, 0)$, which is extracted from a least-square fit of the normalized scattering function around $\omega = 0$. This quantity has units of inverse energy and it is a function of $D_{n\mathrm{D}}Q^2$ and H. Further, it is possible to define a dimensionless quantity $S^M(Q, 0) = S(Q, 0)\pi D_{n\mathrm{D}}Q^2$, which, as a function of α, follows a master curve *independent* of $D_{n\mathrm{D}}$ and Q. The shape of the master curve is purely determined by the type of motion probed (i.e., dimensionality and, if two families of moving atoms are present, the proportion of moving and static atoms) and the shape of the resolution function. The dependence on $D_{n\mathrm{D}}$ and Q is lifted because both α and $S^M(Q, 0)$ are functions of the ratio $D_{n\mathrm{D}}Q^2/H$ and thus are dimensionless quantities. The master curve reflects the overall relationship between the maximum and the width of the resolution-broadened scattering function as the experimental resolution increases.

For the simpler case of Lorentzian resolution (of HWHM equal to H_L), the master curves for 3D and powder-averaged 2D motion have been derived by Lechner [23]. They are $S^M_{3\mathrm{D}}(Q, 0) = \alpha$ and $S^M_{2\mathrm{D}}(Q, 0) = \frac{\alpha^{0.5}}{2} \ln\frac{1+1/\alpha^{0.5}}{|1-1/\alpha^{0.5}|}$ respectively. For the case of Gaussian resolution (of HWHM equal to H_G) we derive, on the basis of [24], $S^M_{3\mathrm{D}}(Q, 0) = \sqrt{\pi}\kappa e^{\kappa^2} erfc(\kappa)$, where $\kappa = \frac{\alpha\sqrt{\ln 2}}{1-\alpha}$. For the powder-averaged 2D motion and Gaussian resolution, we used instead a numerical convolution of $S^{\mathrm{model}}(Q, \omega)$, the predicted signal from the diffusing atom, and $R(\omega)$, the resolution function, to generate the theoretical curve that $S^M_{2\mathrm{D}}(Q, 0)$ should follow.

Figure 2 features the theoretical master curves together with the experimental data we obtained for water confined in a clay and bulk water for a Gaussian type resolution (H_G) varying between 150 μeV and 5 μeV. The main feature is the previously mentioned divergence of the master curves for powder-averaged two-dimensional motion as α tends to 1, case of infinite resolution.

To obtain the experimental data in Fig. 2, the $S(Q, \omega)$ signal (after background subtraction) was at first normalized, such that $\int S(Q, \omega)d\omega = 1$ for each Q. (The integral intensity of $S(Q, \omega)$ was determined from the modeling of the quasielastic zone, between 1.5 meV on the neutron energy gain side and a limit on the neutron energy loss side, determined by the incident neutron energy. The integral intensity served as the normalization factor. It agreed well with a simple integration of $S(Q, \omega)$.) Thereafter we conserve, for each normalized $S(Q, \omega)$, only a set of three values: H_G, Q and $S(Q, 0)$. We use 48 of these sets for the case of bulk water: 6 wave-vectors (0.5, 0.6, 0.7, 0.8, 0.9 and 1.0 Å^{-1}) measured at 8 resolutions ($H_G = 150$, 100, 75, 50, 37.5, 25, 15 and 5 μeV) and 40 sets for the case of water in clay: 5 wave-vectors (0.6, 0.7, 0.8, 0.9 and 1.0 Å^{-1}) measured at the above 8 resolutions. All 48 sets

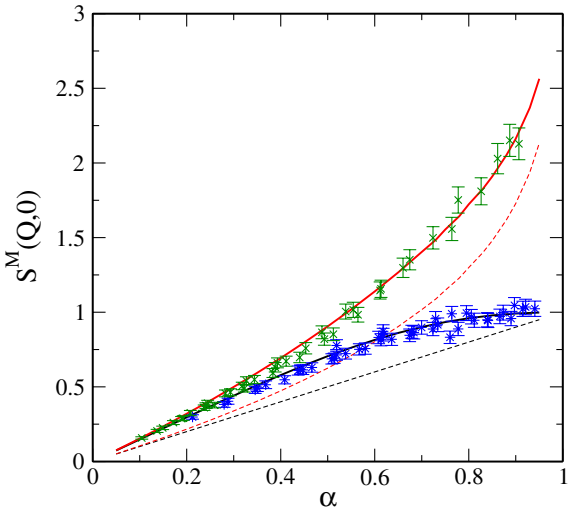

FIG. 2 (color online). $S^M(Q,0)$ $(=S(Q,0)\pi D_{n\mathrm{D}}Q^2)$versus α $(=D_{n\mathrm{D}}Q^2/(D_{n\mathrm{D}}Q^2+H))$, for 3D (isotropic) and powder-averaged 2D motion. For 3D motion, we show the theoretical prediction (master curve) in case of Gaussian resolution (black line) and a corresponding experimental data set collected for bulk water (blue *). For powder-averaged 2D motion, the master curve in case of Gaussian resolution (red line) is accompanied by a set of experimental data for water confined in a synthetic clay (green ×). The analogous master curves in case of 3D and powder-averaged 2D signal combined with Lorentzian resolution are shown as dashed lines. Note that the master curves for Lorentzian resolution are consistently below those for Gaussian resolution, due to the Gaussian function being more peaked at its center.

for bulk water were fitted *simultaneously* to the master curve of 3D diffusion (for the case of Gaussian resolution), with the diffusion coefficient as a sole free parameter. We obtain a diffusion coefficient of 2.4×10^{-9} m^2 s^{-1}, in agreement with the value obtained from the analysis of the quasielastic broadening and of course other independent techniques, e.g., [25]. The 40 sets for water in clay could not be satisfactorily adjusted to the form of the 3D master curve (even master curves for 3D motion with a proportion of immobile atoms), they follow the powder-averaged 2D master curve, corresponding to a diffusion coefficient of $D_{2\mathrm{D}}=0.73\times10^{-9}$ m^2 s^{-1} (again in agreement with the quasielastic broadening analysis). This evidence for the two-dimensional nature of water motion in the model clay system is compelling as it encompasses a simultaneous test across a wide range of experimental resolutions.

We have presented a clear signature of the two-dimensional nature of water diffusion in a powder sample of a synthetic hectorite, a model clay. The conventional modelling of the quasielastic broadening at a single resolution gives, even with the simplest (isotropic) model applied to atomic motion in a complex system, a correct order of magnitude for the diffusion coefficient. The analysis presented here goes further. Using simultaneously information from a wide range of experimental resolutions, it yields unambiguous information on the dimensionality of diffusion, by concentrating on the most pertinent part of the experimentally measured scattering function: the intensity at zero energy transfers. Considering the current advances in scattering techniques (higher signal intensity, wider ranges of resolution), this type of extended analysis seems routinely feasible and highly desirable. Dimensionality is an indicator of the mechanism of diffusion, it informs us about the local geometry a diffusing atom explores within a complex matrix. The structure of the matrix itself might already suggest this, but it is often not sufficient. Determining the dimensionality of the diffusion process is thus of great value.

We thank Josef Breu for providing samples of synthetic hectorite and José Teixeira for insightful comments.

*natalie.malikova@cea.fr

[1] B. C. H. Steele and A. Heinzel, Nature (London) **414**, 345 (2001).
[2] E. Kendrick *et al.*, Nature Mater. **6**, 871 (2007).
[3] A. I. Kolesnikov *et al.*, Phys. Rev. Lett. **93**, 035503 (2004).
[4] F. Salles *et al.*, Phys. Rev. Lett. **100**, 245901 (2008).
[5] *Handbook of Clay Science*, edited by F. Bergaya, B. K. G. Theng, and G. Lagaly (Elsevier, New York, 2006).
[6] B. Smit and T. L. M. Maesen, Nature (London) **451**, 671 (2008).
[7] L. Mirny, Nature Phys. **4**, 93 (2008).
[8] C. Loverdo *et al.*, Nature Phys. **4**, 134 (2008).
[9] M. McCloskey and M. Poo, J. Cell Biol. **102**, 88 (1986).
[10] M. Castro *et al.*, Europhys. Lett. **69**, 770 (2005).
[11] H. Jobic and D. N. Theodorou, Microporous Mesoporous Mater. **102**, 21 (2007).
[12] E. Mamontov, J. Chem. Phys. **121**, 9087 (2004).
[13] H. Jobic, J. Mol. Catal. A: Chem. **158**, 135 (2000).
[14] E. J. M. Hensen and B. Smit, J. Phys. Chem. B **106**, 12 664 (2002).
[15] J. Breu *et al.*, Chem. Mater. **13**, 4213 (2001).
[16] N. Malikova *et al.*, J. Phys. Chem. C **111**, 17603 (2007)
[17] M. Bée, *Quasi-Elastic Neutron Scattering: Principles and Applications in Solid State Chemistry, Biology and Material Science* (Adam Hilger, Bristol and Philadelphia, 1988).
[18] L. Liu, A. Faraone, and S.-H. Chen, Phys. Rev. E **65**, 041506 (2002).
[19] J. Teixeira *et al.*, Phys. Rev. A **31**, 1913 (1985).
[20] J. Ollivier *et al.*, Physica (Amsterdam) **350B**, 173 (2004).
[21] A. J. Dianoux, F. Volino, and H. Hervet, Mol. Phys. **30**, 1181 (1975).
[22] P. L. Hall and D. K. Ross, Mol. Phys. **36**, 1549 (1978).
[23] R. E. Lechner, Solid State Ionics **77**, 280 (1995).
[24] J. I. Langford, J. Appl. Crystallogr. **11**, 10 (1978).
[25] M. Holtz, S. R. Heil, and A. Sacco, Phys. Chem. Chem. Phys. **2**, 4740 (2000).